Construction and Building Materials 497 (2025) 143936

Contents lists available at ScienceDirect

Construction and Building Materials

journal homepage: www.elsevier.com/locate/conbuildmat

Analysis of the chemical, rheological, performance and durability properties of highly polymer-modified bitumen produced at large scale

Sara Carlucci, Lorenzo Paolo Ingrassia *, Simona Sabbatini, Andrea Graziani, Francesco Canestrari

Università Politecnica delle Marche, Via Brecce Bianche, Ancona 60131, Italy

ARTICLE INFO

Keywords:
Pavement
Asphalt
Polymer modification
Styrene polymer
Vinyl group
Highly modified asphalt (HiMA)
Polymer-modified bitumen (PMB)

ABSTRACT

New styrene polymers with high vinyl content in polybutadiene have been recently introduced for bitumen modification. These polymers can potentially ensure higher resistance to oxidation, heat and UV radiation and better compatibility with bitumen compared to conventional SBS (styrene-butadiene-styrene) polymers. Therefore, the polymer content in bitumen can be increased (currently up to 9 %) to produce the so-called *highly polymer-modified bitumen* (HPMB). Among the limited studies available, most of them investigate laboratory-prepared HPMBs, which may not be representative of large-scale production. Conversely, the studies investigating HPMBs produced at an industrial scale often lack detailed binder composition data, limiting the interpretability and generalizability of the results. To address these limitations, the objective of this study is to characterize the chemical, rheological, performance and durability properties of an HPMB currently under development for use in Italian motorway pavements ("HPMB_A") and compare this binder with a reference PMB and two commercially available HPMBs. PMB and HPMB_A were produced at large scale using the same base binder and following the same procedure. These four binders were subjected to an extensive laboratory characterization. The results indicate that the HPMBs behave like a "rubber" modified with bitumen rather than a modified bitumen, which leads to significantly improved performance and aging resistance. However, the adhesive properties of HPMBs can be lower than PMB because of the volumetric predominance of the polymer over the bitumen. Moreover, due to the complexity of these binders, common tests and performance criteria adopted for conventional bitumen may not be fully adequate for HPMBs.

1. Introduction

In recent decades, to cope with the continuous increase in traffic volumes and loads and to adapt road pavements to more aggressive weather conditions, polymer-modified bitumen (PMB) has been increasingly used in pavements instead of neat bitumen [1]. To date, the most widely used polymers for modifying bitumen are the SBS (styrene-butadiene-styrene) polymers. They consist of discontinuous polystyrene domains, which provide stiffness, linked by polybutadiene chains, which provide elasticity. No chemical reaction occurs between bitumen and SBS polymer, meaning that only a physical blending takes place [1,2]. In this reversible process, the polystyrene domains absorb the light components of bitumen (maltenes), causing the polymer to swell (up to 9 times its initial volume) and thus stiffening the binder. Therefore, the SBS content is typically limited to 3–4 % by weight to avoid the phase inversion between bitumen and polymer [1–3].

However, PMBs present some drawbacks, including storage stability issues. In fact, at typical storage temperatures, polymer and bitumen tend to separate, with the polymer migrating upwards. In addition, SBS PMBs have relatively poor resistance to heat, oxidation, and UV radiation due to the presence of highly reactive C═C double bonds in the main chain of polybutadiene [1].

To address the above limitations, new styrene polymers with high vinyl content in the polybutadiene have been recently introduced. Thanks to a different polymerization process of butadiene, in these polymers the highly reactive C═C double bonds of polybutadiene are located in the side chains instead of the main chain. This structural change potentially reduces the exposure to degradation factors like oxidation, heat, and UV radiation (the main polymer chain remains intact) [4,5]. Additionally, for the same molecular weight, the polymer

* Corresponding author.
E-mail addresses: s.carlucci@pm.univpm.it (S. Carlucci), l.p.ingrassia@pm.univpm.it (L.P. Ingrassia), s.sabbatini@univpm.it (S. Sabbatini), a.graziani@univpm.it (A. Graziani), f.canestrari@univpm.it (F. Canestrari).

https://doi.org/10.1016/j.conbuildmat.2025.143936
Received 7 July 2025; Received in revised form 5 September 2025; Accepted 4 October 2025

chains are shorter, possibly improving compatibility with bitumen and reducing the viscosity of the modified binder [4,6]. The compatibility can be further enhanced by the high reactivity of the high-vinyl polymers, which promotes also some chemical reactions between polymer and bitumen (grafting) [4]. Therefore, styrene polymers with high vinyl content enable a higher polymer dosage in bitumen. At present, 9 % is generally considered a maximum feasible value from both technical and economic perspectives [7]. The final product obtained in this way is commonly referred to in the literature as *highly polymer-modified bitumen* (HPMB) or *highly modified asphalt* (HiMA).

The limited studies available in the literature confirm that HPMBs can generally offer improved performance, better storage stability, and higher resistance to aging and oxidation with respect to conventional PMBs. Islam et al. [8] and Kumar et al. [9] compared four types of styrene polymers. These studies confirmed that diblock styrene polymers with high vinyl content are characterized by lower molecular weight with respect to conventional SBS polymers, thus leading to a modified binder with lower viscosity. Singh et al. [10] studied six polymers to evaluate the influence of physical structure and chemical composition on the thermal stability of binders modified with different polymer contents. They found that high-vinyl polymers exhibited significantly better storage stability and lower thermal degradation than the other polymers, even after prolonged storage at 180 °C. Habbouche et al. [11] studied four binders, considering two base bitumens and two types of styrene polymers, i.e., one for the traditional PMB modification and one high-vinyl polymer for HPMB modification. They found that, for the same base bitumen, HPMBs had a much wider useful temperature interval and greater aging resistance compared to PMBs. Rivera et al. [12] compared one PMB and one HPMB provided by the Florida Department of Transportation. Even in this case, the HPMB was characterized by a wider useful temperature interval compared to the PMB, along with reduced time- and temperature-dependence. Elwardany et al. [13] investigated two PMBs and four HPMBs provided by four different suppliers located in Florida and Virginia. It was found that, compared to the PMBs, the HPMBs were characterized by lower stiffness modulus and higher phase angle (more viscous response) at intermediate and high frequencies (i.e., intermediate and low temperatures) as well as higher stiffness modulus and lower phase angle (more elastic response) at low frequencies (i.e., high temperatures), potentially improving the performance against rutting, fatigue and thermal cracking. Multiple Stress Creep and Recovery (MSCR) data confirmed an elastic recovery of about 100 % for the HPMBs at high temperatures. Even in this study, the HPMBs exhibited greater aging resistance than the PMBs.

However, in most of the above studies [8–11], the HPMBs were prepared in the laboratory, which may not be sufficiently representative of actual large-scale production. Instead, in the studies that examine HPMBs produced at an industrial scale [12,13], the binder composition (i.e., base bitumen, polymer type and dosage) is typically undisclosed, which complicates the interpretation and generalization of the results obtained.

The analysis of the literature highlights that few data are currently available, which need to be confirmed or disproved to fully understand the potential and drawbacks of HPMBs, as these are relatively new materials. In addition, there is a lack of data on HPMBs produced at large scale with known composition. To address these limitations, the objective of this study is to characterize the chemical, rheological, performance and durability properties of an HPMB currently under development for use in Italian motorway pavements ("HPMB_A") and to compare this binder with a reference PMB and two HPMBs available on the market. PMB and HPMB_A were produced at large scale using the same base binder and following the same procedure. These binders were subjected to an extensive laboratory characterization.

2. Materials and methods

2.1. Materials

Four binders were investigated in this study:

- A reference bitumen modified with 3.8 % of SBS polymers, routinely used in asphalt mixtures for Italian motorway pavements, coded as "PMB".
- A highly modified bitumen with 7.5 % of styrene polymers under development, coded as "HPMB_A".
- A highly modified bitumen with styrene polymers, produced in Northern Europe and available on the market, coded as "HPMB_O".
- A highly modified bitumen with styrene polymers, produced in Southern Europe and available on the market, coded as "HPMB_V".

To produce the reference PMB, a 70/100 base bitumen and a radial SBS polymer with a styrene content of 31 % were used. HPMB_A was produced with the same base bitumen (70/100) plus styrene polymers with a high vinyl content (> 35 %) and a styrene content between 30 % and 34 %. The adoption of a 7.5 % polymer content for HPMB_A was based on several practical considerations, including the polymer manufacturer's recommendations, comparisons with existing commercial products and literature studies, as well as the need to limit material costs. The large-scale production process followed for HPMB_A was the same as for PMB. Instead, for HPMB_O and HPMB_V, the base bitumen as well as the type and exact dosage of polymers are not declared by the respective producers. The empirical properties of the binders measured in the laboratory are shown in Table 1. For HPMB_A, the storage stability was evaluated at the asphalt plant after its production, yielding satisfactory results (0.5 °C difference in the softening point between the top and bottom parts after the tube test).

2.2. Experimental program

The experimental program involved short-term and long-term aging of the binders, chemical analysis, rheological tests and adhesion tests. The chemical analysis was based on Fourier Transform Infrared Spectroscopy (FTIR) and aimed at investigating the chemical fingerprint of the binders, their aging susceptibility and the possible polymer degradation. The viscosity, linear viscoelastic behaviour, fatigue performance, permanent deformation resistance and adhesion properties of the binders were evaluated through Brookfield viscometer tests, Frequency Sweep (FS) tests, Linear Amplitude Sweep (LAS) tests, MSCR tests and Binder Bond Strength (BBS) tests, respectively. The Performance Grade (PG) of the binders was also determined based on the results of Dynamic Shear Rheometer (DSR) tests and Bending Beam Rheometer (BBR) tests. For all tests, three replicates were performed, except for the BBS test, for which at least five replicates were carried out. Table 2 summarises the experimental program.

2.3. Test methods

2.3.1. Aging protocols

Short-term aging was simulated through the Rolling Thin Film Oven Test (RTFOT) equipment at the standard temperature of 163 °C for 75 min [14]. Long-term aging was simulated through the Pressure Aging Vessel (PAV). Specifically, binders already aged with the RTFOT were subjected to a pressure of 2.1 MPa at 100 °C for 20 h, according to EN

Table 1
Empirical properties of the binders.

Property	PMB	HPMB_A	HPMB_O	HPMB_V
Penetration at 25 °C (0.1 mm)	32	31	53	61
Softening point by Ring and Ball (°C)	74.8	75.2	87.3	79.7

Table 2
Experimental program.

Aging Level	FTIR	Viscosity	FS	BBR	LAS	MSCR	BBS
Unaged	x	x	x			x	x
Short-term aged	x		x		x	x	
Long-term aged	x		x	x	x		

14769 [15].

Hereafter, the suffixes "UN" (unaged), "ST" (short-term aged) and "LT" (long-term aged) are added to the binder codes (Section 2.1) to denote the aging condition.

2.3.2. Fourier Transform Infrared spectroscopy

Fourier Transform Infrared (FTIR) spectroscopy was performed in transmission mode (i.e., the infrared light passed through the specimen) at room temperature. Measurements were taken in the wavenumber range between 500 and 4000 cm^{-1}, with a spectral resolution of 4 cm^{-1}. Each spectrum was acquired from a single specimen after 16 scans. To prepare the specimens, a small amount of binder was dissolved in chloroform ($CHCl_3$), and the resulting solution was applied to sodium chloride (NaCl) plates. Once the solvent evaporated, a thin binder film was obtained and subjected to the analysis. For each binder and aging condition, an average spectrum was determined. The average spectra were then analysed using an integration method that allowed to identify the areas under the most relevant peaks through a tangential approach [16].

2.3.3. Viscosity tests

The viscosity was determined at four temperatures (115, 135, 160 and 180 °C) using a Brookfield viscometer [17]. For each temperature, viscosity was measured at five different shear rate values. The viscosity value considered for further analysis corresponds to a torque close to 50 % of the instrument capacity.

2.3.4. Frequency sweep tests

Frequency sweep tests were carried out using a DSR with 8 mm (2 mm gap) and 25 mm (1 mm gap) parallel plate configurations, according to EN 14770 [18]. The investigated temperature range was from 4 °C to 88 °C, with a 6 °C step. Nine frequencies were analysed at each test temperature, considering the range from 0.159 Hz to 15.9 Hz with a fixed logarithmic frequency increase. A shear strain of 0.1 % was applied in all cases, ensuring that all materials were tested within the linear viscoelastic domain.

The frequency sweep tests provided the complex modulus, i.e., the complex modulus norm $|G^*|$ and the phase angle δ. The data obtained at different temperatures and frequencies were used to develop the master curves at the reference temperature of 34 °C. The shift factors were calculated using the closed from t-T-P Shifting (CFS) algorithm [19], and the thermo-dependence of the shift factors was modelled using the Williams, Landel and Ferry (WLF) equation [20].

The shifted experimental data were fitted using the modified CAM (Christensen-Anderson-Marasteanu) model [21] characterized by the following general formulation:

$$|G^*| = G_e + \frac{G_g - G_e}{\left[1 + (f_c/f')^k\right]^{m_e/k}} \quad (1)$$

where f' is the reduced frequency; G_e and G_g are the rubbery modulus ($f' \to 0$) and glassy modulus ($f' \to \infty$), respectively; f_c is the crossover frequency, i.e., the frequency at which the storage modulus ($G' = |G^*| \cdot \cos\delta$) is equal to the loss modulus ($G'' = |G^*| \cdot \sin\delta$); k and m_e are dimensionless shape parameters. The rheological indices R and R' were also determined, representing the distance between G_g and $|G^*(f_c)|$ and the distance between G_e and $|G^*(f'_c)|$, respectively (f'_c is the reduced frequency at which the asymptotes G_e and m_e intercept) [21].

For the modelling, G_e was estimated from the experimental data (Black diagram), and f_c was determined as the reduced frequency corresponding to $\delta = 45°$ (at which $G' = G''$). The parameters G_g, k and m_e were optimized by minimizing the error between the model and the shifted experimental data in terms of $\log|G^*|$ (with $G_g \geq 10^9$ MPa [22]). R, f'_c and R' were finally calculated (the latter two only for the binders with $G_e \neq 0$).

2.3.5. Bending beam rheometer tests

BBR tests were performed in accordance with EN 14771 [23] to evaluate the stiffness and creep properties of the binders at low temperatures. The tests were carried out at constant temperature by applying a constant load of 980 mN for 240 s, during which the load and the deflection at the centre of the specimen (beam with 6.4 mm thickness, 12.7 mm width, 127 mm length) were monitored. The behaviour of the material was then evaluated by considering the flexural creep stiffness and the m-value (i.e., the absolute value of the slope of the logarithm of the stiffness vs. the logarithm of time, representative of the material's ability to relax the applied stress) obtained at $t = 60$ s (denoted as S_{60} and m_{60}, respectively).

The four binders were tested at different temperatures. Specifically, the reference bitumen (PMB) was tested at –6 °C and –12 °C, HPMB_A at –12 °C and –18 °C, HPMB_O and HPMB_V at –12 °C, –18 °C and –24 °C.

2.3.6. Performance Grade determination

The PG of the binders was determined based on DSR data (high-temperature and intermediate-temperature behaviour) and BBR data (low-temperature behaviour), in accordance with AASHTO M 320 [24]. Using the PG classification system, the maximum T_{max} and minimum T_{min} admissible service temperatures were determined for all binders.

In addition to the PG, the continuous PG was also determined, i.e., the actual T_{max} and T_{min} temperatures at which the high-temperature and low-temperature criteria are met (regardless of the 6 °C classes reported in the standard AASHTO M 320 [24]).

Moreover, in addition to the classical verification of the SHRP fatigue parameter ($|G^*| \cdot \sin\delta \leq 5000$ kPa) at the temperature $T_{fatigue} = (T_{max} + T_{min})/2 + 4$ °C, an additional fatigue verification was carried out by considering the Glover-Rowe Parameter $GRP = |G^*| \bullet (\cos\delta)^2/\sin\delta$ (which should be lower than 5000 kPa). In fact, according to a recent study [25], this parameter better correlates with the fatigue behaviour of the asphalt mixture than the $|G^*| \cdot \sin\delta$ parameter. GRP was calculated for the long-term aged binders from the DSR data at 1.59 Hz and a temperature T_{GRP} defined as a function of the binder T_{min}.

2.3.7. Linear amplitude sweep tests

LAS tests were carried out using the DSR with the 8 mm parallel plate configuration (2 mm gap), according to AASHTO T 391 [26], at 20 °C (typical intermediate service temperature in warm climates).

The test included an initial frequency sweep phase to evaluate the undamaged binder properties, and an amplitude sweep phase to evaluate the damaged properties. In the first phase, a constant sinusoidal shear strain of 0.1 % was applied and the viscoelastic properties (norm of complex modulus and phase angle) were measured at 12 frequencies (between 0.2 Hz and 30 Hz). In the second phase, the frequency was fixed at 10 Hz, whereas the shear strain amplitude was increased from 0.1 % to 30 % in 31 steps (each one with a duration of 10 s). During this phase, the values of peak shear stress, peak shear strain, norm of complex modulus and phase angle were recorded. After the test, the specimen was observed to determine whether the failure was cohesive (required failure) or adhesive (undesired failure).

The results were analysed according to the Viscoelastic Continuum Damage (VECD) theory, as indicated in AASHTO T 391 [26]. The relationship between the loss modulus $|G^*| \cdot \sin\delta$ and the damage accumulation parameter S (defined in Eq. 2) was derived. This relationship, known as the damage characteristic curve, describes the integrity of the

binder (C) as a function of the damage level and can be fitted with the power law provided in Eq. 3.

$$S = \sum_{i=1}^{N} \left[\pi I_D \gamma_0^2 \bullet \left(|G^*| \bullet \sin\delta_{i-1} - |G^*| \bullet \sin\delta_i\right)\right]^{\frac{\alpha}{1+\alpha}} \bullet (t_i - t_{i-1})^{\frac{1}{1+\alpha}} \quad (2)$$

where i is the i-th measurement point; N is the total number of measurement points; I_D is the value of $|G^*|$ at the beginning of the interval in which the strain value is 1 % (MPa); γ_o is the strain applied at the i-th step (%); t is the test time (s); α expresses the damage growth rate and is derived from the initial frequency sweep phase.

$$C = |G^*| \bullet \sin\delta = \quad C_0 - C_{11} \bullet (S)^{C_{12}} \quad (3)$$

where C_o is the average value of $|G^*| \bullet sin\ \delta$ obtained from the interval in which $\gamma = 0.1$ % (with the material still intact); C_{11} and C_{12} are the coefficients derived from the fitting.

The fatigue curve of the binder was then determined as follows:

$$N_f = \quad A_{35} \bullet (\gamma)^{-B} \quad (4)$$

where N_f is the fatigue life; γ is the shear strain amplitude; A_{35} and B are parameters that quantify the fatigue life for a strain amplitude of 1 % and the strain sensitivity of the binder, respectively. To calculate the parameter A_{35}, a value of S at failure corresponding to a 35 % reduction of C_0 was considered according to AASHTO T 391 [26].

2.3.8. Multiple stress creep and recovery tests

MSCR tests were performed using the DSR with the 25 mm parallel plate configuration (1 mm gap), in accordance with AASHTO T 350 [27], at a typical high service temperature of 70 °C.

The test consisted in the application of 30 load cycles, each one characterized by a creep phase (with a duration of 1 s) followed by a recovery phase (with a duration of 9 s). The first 20 cycles involved the application of a stress level of 0.1 kPa, whereas a stress level of 3.2 kPa was applied in the last 10 cycles. The non-recoverable creep compliance (J_{nr}) and the percent strain recovery (R) were then determined by considering only the last 20 cycles, i.e., 10 cycles at 0.1 kPa and 10 cycles at 3.2 kPa.

2.3.9. Binder bond strength tests

BBS tests were conducted in accordance with AASHTO T 361 [28] to assess the adhesive/cohesive properties and moisture susceptibility of different binder-aggregate systems.

Using a modified Pneumatic Adhesion Tensile Testing Instrument (PATTI), an increasing pulling force was applied to a small binder sample adhering onto the aggregate substrate through a pull-stub, until failure occurred. The pull-off tensile strength (POTS) of the system was then calculated and the type of failure (cohesive, adhesive or hybrid) was determined by observing where the failure occurred, i.e., within the binder (cohesive, C), at the binder/substrate interface (adhesive, A) or as a combination of both (hybrid, C/A). The pull-stubs used had an external diameter of 12.7 mm, an internal diameter of 12.5 mm (i.e., diameter of the binder-aggregate contact area), and a 0.3 mm thick edge (i.e., thickness of the binder sample). The specimens were prepared by applying 0.08 g of binder onto the head of the pull-stub. The pull-stub was then placed in an oven for approximately 10 min at 160 °C for PMB and HPMB_A, 170 °C for HPMB_O and 180 °C for HPMB_V. Two types of aggregate substrates (limestone and basalt) and two aggregate conditions (virgin/uncoated and pre-coated with SBS polymer modified bitumen) were investigated. The pre-coated condition simulated reclaimed asphalt (RA) aggregates [29]. The bituminous film present on the coated aggregates was aged in accordance with AASHTO R 30 [30], i.e., by considering an oven aging at 135 °C for 4 h and then at 85 °C for 120 h. Moreover, two types of specimen conditioning were studied, i.e., dry (24 h at 25 °C) and wet (24 h in water at 40 °C followed by 1 h in air at 25 °C).

3. Results and analysis

3.1. FTIR spectra

3.1.1. General observations

The average spectra of the four binders in unaged and long-term aged conditions are shown in Fig. 1a and 1b, respectively. The peaks of interest are highlighted in Fig. 1 and reported in Table 3.

The peaks at wavenumbers 966 cm^{-1} and 699 cm^{-1}, corresponding to the bending of the *trans* C=C bond in polybutadiene and the bending of the C-H bond in polystyrene respectively, confirm the presence of styrene polymers in the reference bitumen PMB as well as in the three HPMBs. Instead, the peak at 908 cm^{-1}, which is observed only for the three HPMBs, corresponds to the bending of the *vinyl* C=C bond in polybutadiene resulting from the 1,2-addition polymerisation process [11].

3.1.2. Estimation of the polymer content

The polymer content in the four binders was estimated using Eq. (5) [31], which derives from a calibration curve and considers the height of the peaks at 699 cm^{-1} (H_{699}) and 1376 cm^{-1} (H_{1376}):

$$\%P = \frac{0.000251 \bullet (H_{699}/H_{1376})}{0.05759} \quad (5)$$

Fig. 2 confirms the polymer contents for PMB and HPMB_A (about 3.5 % and 7.5 %, respectively) and indicates a polymer content around 7.5 % for HPMB_O, even higher for HPMB_V. It should be noted that, for HPMB_V, the increase in the polymer content with aging observed in Fig. 2 may also be a consequence of the non-representativeness and/or heterogeneity of the material recovered after RTFOT and PAV, which emerged also from the rheological tests (see Section 3.3).

3.1.3. Aging susceptibility

To assess the aging susceptibility of the binders, the peaks at 1030 cm^{-1} and 1700 cm^{-1} , associated with the stretching of S=O bonds and C=O bonds respectively, were considered. Specifically, two indices (I_{SO} and I_{CO}) were derived based on the calculation of the areas corresponding to the peaks of interest (A_{1030} and A_{1700}). In order to minimise the differences between different specimens, the above areas were normalised to the sum of the areas of the aliphatic groups at 1460 cm^{-1} and 1376 cm^{-1} ($A_{1460} + A_{1376}$), corresponding to the bending of the CH_2 and CH_3 bonds, respectively. These aliphatic groups are normally not affected by oxidation [32]. The expressions of the I_{SO} and I_{CO} indices are given in Eqs. (6) and (7):

$$I_{SO} = \frac{A_{1030}}{A_{1376} + A_{1460}} \quad (6)$$

$$I_{CO} = \frac{A_{1700}}{A_{1376} + A_{1460}} \quad (7)$$

Fig. 3a shows the evolution of the I_{SO} index for the four binders at the three aging levels. As regards the formation of S=O bonds, PMB is more sensitive to aging as compared to the HPMBs, both in the short and in the long term. Among the HPMBs, HPMB_O is less susceptible to short-term aging but highly susceptible to long-term aging. In contrast, HPMB_A and HPMB_V are more sensitive to short-term aging than HPMB_O, but no new S=O bonds are formed after long-term aging.

Fig. 3b depicts the values of the I_{CO} index. This index is null in unaged and short-term aged conditions (short-term aging with RTFOT does not lead to the formation of C=O bonds). PMB is more affected by long-term aging as compared to the HPMBs also in terms of C=O bond formation. Among the HPMBs, HPMB_A is the binder most susceptible to the formation of C=O compounds, followed by HPMB_V and finally HPMB_O.

To further explore this aspect and directly compare the aging sus-

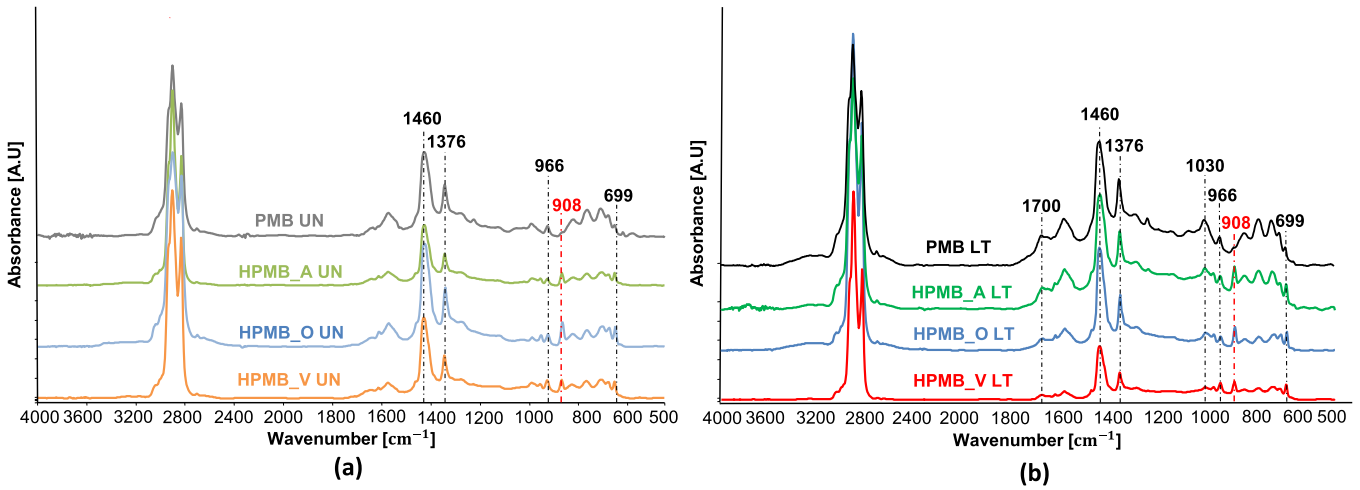

Fig. 1. FTIR spectra of (a) unaged binders, (b) long-term aged binders.

Table 3
Peaks of interest in the FTIR spectra.

Wavenumber [cm^{-1}]	Vibration	Area
699	Bending of C-H bond (polystyrene)	A_{699}
908	Bending of *vinyl* C═C bond (polybutadiene)	A_{908}
966	Bending of *trans* C═C bond (polybutadiene)	A_{966}
1030	Stretching of S═O bond (sulfoxides)	A_{1030}
1376	Bending of CH_3 bonds	A_{1376}
1460	Bending of CH_2 bonds	A_{1460}
1700	Stretching of C═O bond (carbonyl groups)	A_{1700}

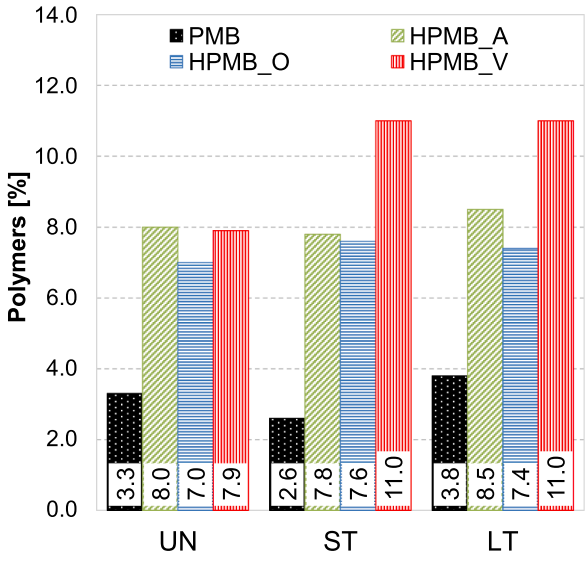

Fig. 2. Estimated polymer content.

ceptibility of the binders, the following aging index (AI_{FTIR}) can be considered [33]:

$$AI_{FTIR} = \frac{(I_{CO} + I_{SO})_{aged}}{(I_{CO} + I_{SO})_{unaged}} \quad (8)$$

From Fig. 3c, it can be observed that, during short-term aging, the HPMBs tend to oxidise slightly less than the reference bitumen PMB (especially HPMB_O). On the other hand, HPMB_O is strongly affected by long-term aging, which leads to an aging index AI_{FTIR} even higher than that observed for the reference bitumen PMB under these conditions. Conversely, HPMB_A and HPMB_V are much less affected by long-term aging than PMB (especially HPMB_V).

The comparison between HPMB_A and PMB in terms of AI_{FTIR}, both presenting the same base bitumen but differing in polymer type and content, reveals that using 7.5 % of styrene polymers with a high vinyl content (HPMB_A) significantly reduces the aging susceptibility as compared to the reference bitumen PMB. This effect stems partly from the higher polymer content and partly from the polymer structure, confirming the benefits of having the chemically reactive C═C double bonds of polybutadiene in the side chains (as in high-vinyl polymers) rather than in the main chain (as in radial SBS polymers).

Moreover, based on the aging behaviour observed for HPMB_O and HPMB_V, it can be hypothesized that HPMB_V contains polymers similar to those in HPMB_A, whereas the polymers in HPMB_O are likely different (e.g., in terms of structure), given the pronounced long-term aging susceptibility of this binder.

3.1.4. Polymer degradation

Following some literature suggestions [11,34,35], other synthetic indices were also derived to assess the possible polymer degradation within the binders. Specifically, four polymer indices were calculated, i.e., PI_{908} (Eq. 9 and Fig. 4a) and $PI_{908/699}$ (Eq. 10 and Fig. 4b) for the HPMBs, PI_{966} (Eq. 11 and Fig. 4c) and $PI_{966/699}$ (Eq. 12 and Fig. 4d) for all binders. The definition of these indices is based on the fact that polybutadiene (characteristic peaks at 966 and 908 cm^{-1}) typically degrades faster than polystyrene (characteristic peaks at 699 cm^{-1}) due to oxidation.

$$PI_{908} = \frac{A_{908}}{A_{1376} + A_{1460}} \quad (9)$$

$$PI_{908/699} = \frac{A_{908}}{A_{699}} \quad (10)$$

$$PI_{966} = \frac{A_{966}}{A_{1376} + A_{1460}} \quad (11)$$

$$PI_{966/699} = \frac{A_{966}}{A_{699}} \quad (12)$$

From Fig. 4, it can be observed that none of these indices shows a clear decrease with the increase of the aging level for the binders HPMB_A and HPMB_V. Conversely, all indices decrease with aging in the case of HPMB_O. The indices PI_{966} and $PI_{966/699}$ also tend to decrease with aging for the reference bitumen PMB. Therefore, these results suggest that PMB and HPMB_O undergo more severe polymer degradation.

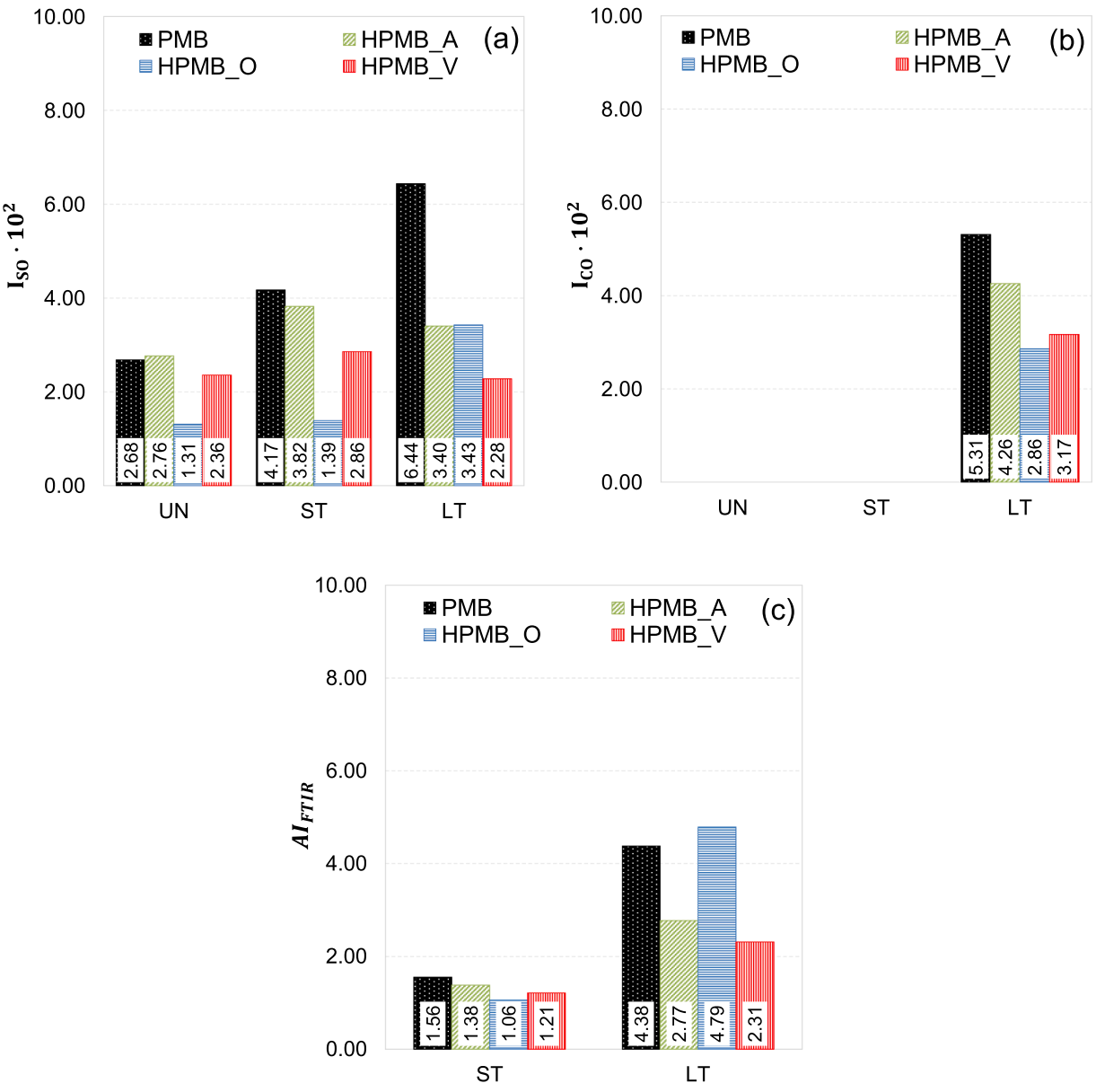

Fig. 3. FTIR indices: (a) I_{SO}, (b) I_{CO}, (c) Aging Index AI_{FTIR}.

3.2. Viscosity

Fig. 5 shows the viscosity of the unaged binders (logarithmic scale) at different temperatures. In the figure, the error bars represent the standard deviation. In general, the HPMBs tend to be more viscous than the reference bitumen except for HPMB_A, which exhibits comparable or even lower viscosity with respect to PMB despite its high polymer content. Considering that the base bitumen is the same for PMB and HPMB_A, this behaviour can be attributed to the fact that the molecular weight of the styrene polymers with high vinyl content used in HPMB_A is lower than that of the radial SBS polymers used in PMB [4,6,8,9]. From the comparison between HPMB_O and HPMB_V, it is observed that HPMB_O tends to be more viscous than HPMB_V at lower temperatures (115 °C), whereas the opposite occurs at high temperatures (160 °C and 180 °C), which denotes a lower temperature-dependence for HPMB_V.

The results obtained suggest that PMB and HPMB_A may have similar workability at typical mixing, transport, laying and compaction temperatures, whereas HPMB_O and HPMB_V may have reduced workability as compared to the reference bitumen. This applies to both hot (T ≈ 170 °C) and warm (T ≈ 130 °C) production of the asphalt mixture. Moreover, the tests highlighted that the hypothesis of Newtonian behaviour is valid for all binders (viscosity does not depend on the shear rate).

3.3. Complex modulus

Fig. 6 shows the Black diagram of the unaged, short-term aged and long-term aged binders, i.e., the raw rheological data plotted on the plane of complex modulus norm (y axis) vs. phase angle (x axis). From this figure, it can be observed that the binders behave differently from each other. In general, the HPMBs exhibit a more complex rheological behaviour as compared to the reference bitumen PMB. This is especially evident for HPMB_A and HPMB_V.

Fig. 7 shows the master curves of the complex modulus norm (experimental data and corresponding modified CAM models) for the binders at all aging levels, determined at the reference temperature of 34 °C. From Fig. 7a, it can be noted that the HPMBs tend to have higher stiffness at low reduced frequencies (i.e., high temperatures) and lower stiffness at high reduced frequencies (i.e., low temperatures) as compared to the reference bitumen PMB, indicating that the

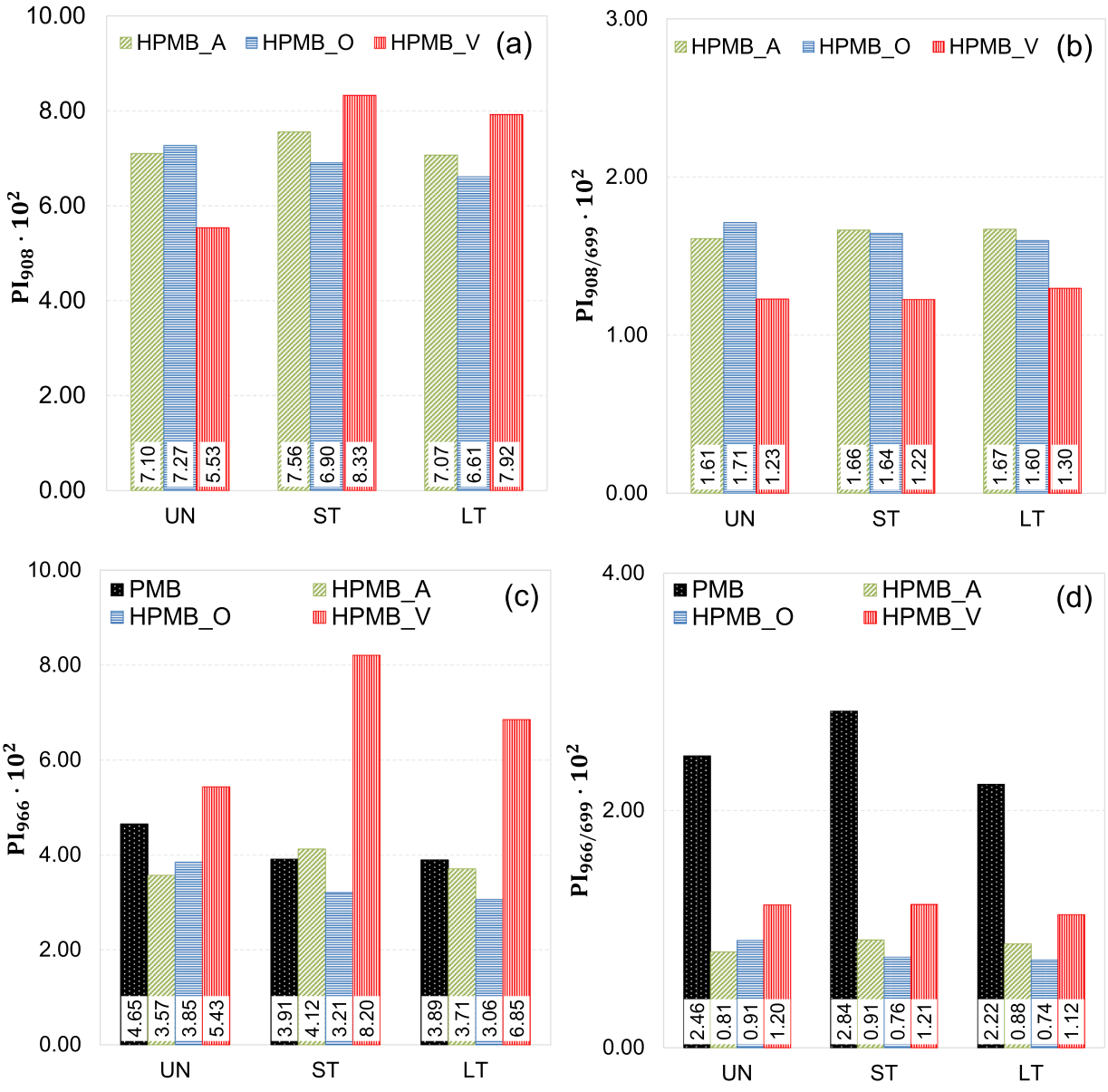

Fig. 4. Polymer Indices: (a) PI_{908}, (b) $PI_{908/699}$, (c) PI_{966}, (d) $PI_{966/699}$.

modification with ad hoc styrene polymers produces the desired effects.

For HPMB_V, and to a lesser extent for HPMB_A, the shifted data tends to form a 'bump' at medium-low reduced frequencies and, as a result, the modified CAM model does not fit the measured data well (Fig. 7a). This behaviour could be due to the fact that, at these frequencies, the properties of the polymer become dominant over the properties of the base bitumen [11]. HPMB_O, instead, exhibits the rubbery asymptote at low reduced frequencies, which is slightly detectable also for PMB (Fig. 7a).

The effect of aging is more evident for the reference bitumen PMB than for the HPMBs. In fact, as shown in Fig. 7b and c, PMB is the stiffest binder in both short- and long-term aging conditions, and its hinted rubbery asymptote in unaged conditions already disappears after short-term aging. Figs. 7b and 7c also show a progressive loss of the rubbery asymptote with aging for HPMB_O. These results are attributable to the degradation of the polymers contained in PMB and HPMB_O, which emerged also from the FTIR tests (Fig. 4). Instead, for HPMB_V and HPMB_A, the 'bump' at medium-low frequencies in the master curve of the complex modulus norm is still observable after aging. However, it should be underlined that, for HPMB_V, some repeatability issues emerged after long-term aging, probably due to the non-representativeness and/or heterogeneity of the material recovered after RTFOT and PAV (as also discussed in Section 3.1). Therefore, it was not possible to derive the master curve for this binder in long-term aged conditions.

Fig. 8 compares the phase angle master curves of the binders at all aging levels. In unaged conditions (Fig. 8a), HPMB_A and HPMB_V show a completely different behaviour as compared to the other binders. In fact, for these two binders, the phase angle master curves show an inverse "N" shape and values tending towards 90° at low reduced frequencies (predominantly viscous response). This behaviour, which is more evident for HPMB_V, is directly related to the 'bump' observed in the complex modulus master curves in Fig. 7a and is likely due to the dominance of the polymer's behaviour at medium-low reduced frequencies [11]. On the other hand, HPMB_O is characterized by a phase angle reduction at low reduced frequencies (also observed for PMB), which leads to a more elastic response with respect to the other binders. At the same time, at high reduced frequencies, HPMB_O shows a higher phase angle compared to the other binders, indicating a more viscous response (desired effects of polymer modification).

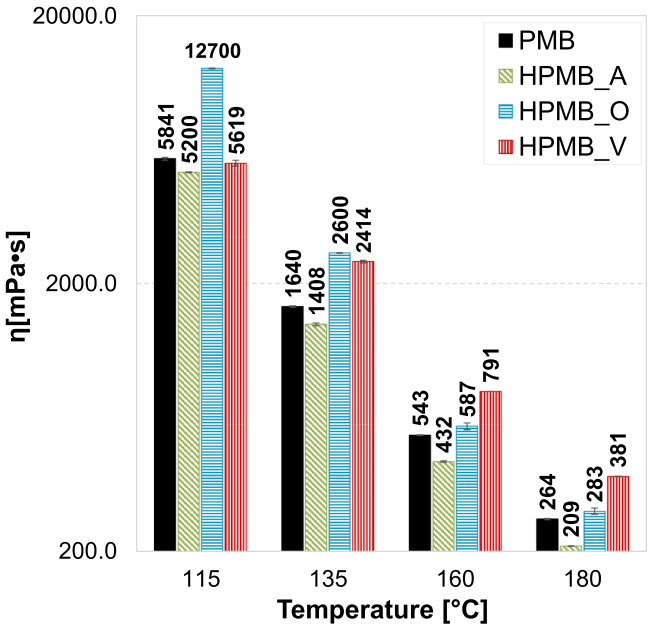

Fig. 5. Viscosity of the binders as a function of temperature.

For PMB, an evident increase in the phase angle at low reduced frequencies is observed after short-term aging (Fig. 8b), which could be indicative of the significant degradation of the SBS radial polymer after the exposure to high temperatures (confirming the FTIR results in Fig. 4c and d). After long-term aging, the downward shift in phase angle reflects the elasticity increase due to the bitumen stiffening (Fig. 8c). For HPMB_O, aging causes a progressive increase in the phase angle at low reduced frequencies. This behaviour, coupled with the loss of the rubbery asymptote in the complex modulus master curve (Fig. 7), is ascribable to the polymer degradation (evidenced by the FTIR results in Fig. 4), which leads to a more viscous response of the material after aging. On the contrary, HPMB_A exhibits a phase angle reduction with aging, which is the typical effect observed for unmodified bitumen, denoting the polymer preservation (in agreement with the FTIR results in Fig. 4) and a more elastic behaviour after aging. Finally, for HPMB_V, short-term aging induces a slight decrease in the phase angle over a wide range of reduced frequencies (long-term aged data not available).

Therefore, the rheological data (as well as the chemical data, see Section 3.1) seem to support the hypothesis that the polymers used in HPMB_A and HPMB_V are similar, whereas those used in HPMB_O are substantially different. Moreover, the rheological behaviour of HPMB_O appears closer to that of the reference bitumen PMB, especially in unaged conditions.

The values of the modified CAM model parameters and the C_1 and C_2 parameters of the WLF equation, obtained by fitting the shift factors calculated with the CFS algorithm, are given in Table 4. For HPMB_O in all aging conditions and for PMB in unaged conditions, which exhibit the rubbery asymptote ($G_e \neq 0$), Table 4 also shows the values of the G_e, f'_c and R' parameters of the modified CAM model. It should also be recalled that, because of the complex rheological behaviour of HPMB_A and HPMB_V, the CAM model does not fit the experimental data well for these materials (see Fig. 7). Consequently, for HPMB_A and HPMB_V, the values of the parameters derived from the modelling cannot be considered as fully representative of the material behaviour.

As regards the effect of aging, it can be observed that for all binders (except HPMB_V) there is a progressive decrease in the crossover frequency f_c as the aging level increases, indicating a greater elastic response of the material after aging. Similarly, the WLF parameters C_1 and C_2 exhibit generally increasing values as the aging level increases, suggesting a reduction in molecular mobility with aging [36,37]. The rheological index R, instead, generally tends to increase with the aging degree for all binders, contrary to expectations (for traditional bitumen, aging typically results in a reduction of R, which denotes a faster transition from predominantly elastic to predominantly viscous behaviour). For HPMB_O, it can be observed that the rubbery modulus G_e decreases as the aging degree increases as a consequence of progressive polymer deterioration. Additionally, the frequency f'_c tends to decrease with aging (like f_c), as does the rheological index R'.

3.4. Low-temperature behaviour

Fig. 9 shows the BBR results obtained on the long-term aged binders, i.e., the average values of S_{60} (Figure 9a) and m_{60} (Fig. 9b). In the figure, the error bars represent the standard deviation. Fig. 9a shows that, considering the same binder, S_{60} (which is representative of the material stiffness) increases as the test temperature decreases (expected result). At the same temperature, the HPMBs are characterised by much lower stiffness values compared to PMB. Specifically, at –12 °C, HPMB_A and HPMB_O exhibit a 51 % and 43 % reduction in stiffness, respectively, compared to the reference bitumen PMB.

Fig. 9b shows that, for a given binder, m_{60} (which indicates the ability of the material to relax the applied stress) decreases as the temperature decreases. At the same temperature, the HPMBs exhibit much higher m_{60} values than the reference bitumen. Specifically, at –12 °C, HPMB_A and HPMB_O exhibit 180 % and 200 % increases in m_{60} values, respectively, compared to the reference bitumen PMB.

For HPMB_V, it was not possible to obtain S_{60} and m_{60} at –12 °C and –18 °C because the specimen deflection exceeded 4 mm. At –24 °C, a very low S_{60} value (Fig. 9a) and a relatively high m_{60} value (Fig. 9b) were obtained. These results are consistent with those obtained from the frequency sweep tests, which showed that the stiffness of HPMB_V is significantly lower than the other binders at high reduced frequencies (Fig. 7).

Therefore, the HPMBs exhibit better performance at low temperatures compared to the reference bitumen PMB.

3.5. Performance Grade

The temperatures T_{max} and T_{min} of the PG and continuous PG are reported in Table 5. The PG results indicate that, when comparing the two binders HPMB_A and PMB (which have the same base bitumen), the use of 7.5 % high-vinyl styrene polymers allows HPMB_A to fall into a higher T_{max} class (82 °C for HPMB_A vs. 76 °C for PMB). For HPMB_V, exceptionally high performance against permanent deformation is observed, as the verification criteria are met even at 88 °C, indicating that T_{max} is higher than 88 °C. Finally, HPMB_O has a T_{max} comparable to that of PMB. Specifically, for HPMB_O, the critical condition is after short-term aging.

In terms of T_{min}, for HPMB_A (T_{min} = –22 °C), there is an improvement of two PG classes with respect to PMB (T_{min} = –10 °C) thanks to the use of 7.5 % high-vinyl styrene polymers. For HPMB_O, produced in Northern Europe, the low-temperature performance is even better (T_{min} = –28 °C). Finally, for HPMB_V, it was not possible to accurately determine T_{min} due to its significant deformability at low temperatures (see Section 3.4), which leads to $T_{min} < -34$ °C.

The continuous PG confirms that, in general, the HPMBs have a higher T_{max} compared to the reference bitumen (except for HPMB_O, which has the same T_{max} as PMB). At low temperatures, the effect of the high polymer modification is even more evident, as all HPMBs are characterised by a much lower actual T_{min} compared to the reference bitumen.

Table 5 also reports the outcomes of the fatigue verifications based on the $|G^*|\bullet\sin\delta$ and GRP parameters. The fatigue verification based on the first criterion ($|G^*|\bullet\sin\delta \leq 5000$ kPa at $T_{fatigue}$) is satisfied for all binders, thus confirming the PG of the binders (76–10 for PMB, 82–22 for HPMB_A, 76–28 for HPMB_O). Regarding the second criterion (GRP

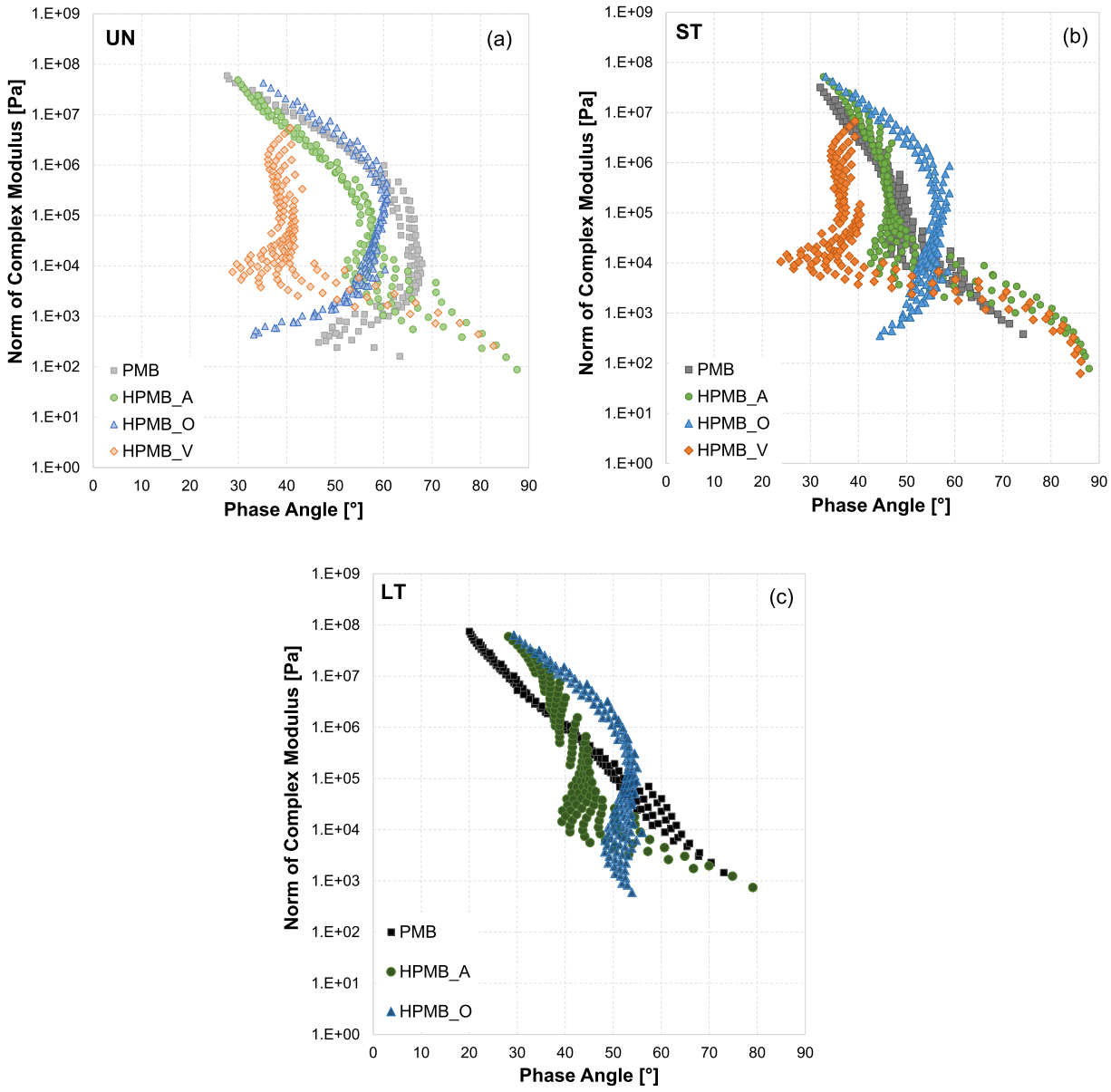

Fig. 6. Black diagram: (a) unaged binders, (b) short-term aged binders, (c) long-term aged binders.

$\leq$ 5000 kPa at T_{GRP}), the verification is largely satisfied for HPMB_A and HPMB_O. Conversely, for PMB, the verification criterion is not met (GRP = 5594 kPa), contrary to what observed from the verification based on the $|G^*|\bullet\sin\delta$ parameter.

3.6. *Fatigue behaviour*

Fig. 10 shows the LAS results for the long-term aged binders, as this condition is normally considered as the most critical for the fatigue performance and similar considerations can be made also for the short-term aged binders. Moreover, Table 6 summarises the values of the damage characteristic curve (C_{11} and C_{12}) and fatigue curve (A_{35} and B) parameters for all binders (short- and long-term aging conditions). It should be emphasized that, for HPMB_V, no reliable results were obtained, as a systematic detachment of the specimen from the DSR plates was observed. This experimental observation indicates that, in the case of HPMB_V, the weak point of the system was the interface between the specimen and the DSR plates, whereas the specimen itself remained almost intact during the test. Therefore, the results obtained for this binder in terms of stress-strain curve and damage characteristic curve are shown in Fig. 10 only for completeness.

Specifically, Fig. 10 shows the stress-strain curve (Fig. 10a), the damage characteristic curve (i.e., the evolution of the material integrity as a function of the damage level, Fig. 10b) and the fatigue curve (i.e., the number of cycles to failure as a function of the applied strain, Fig. 10c). Fig. 10a highlights that the HPMBs show a different stress-strain behaviour with respect to the reference bitumen PMB. Specifically, the curves of the HPMBs show a continuously increasing trend with no apparent peak up to the maximum applied strain of 30 % (in contrast to what is observed for PMB). This result is consistent with the literature [7,38]. A clear difference between PMB and HPMBs can be observed also in terms of damage characteristic curve (Fig. 10b), which indicates that the reference bitumen accumulates more damage during the test (consistently with the specimen failure corresponding to the peak of the stress-strain curve). Furthermore, because of the higher stiffness of PMB (see Fig. 7), its curve is shifted upwards compared to HPMB_A and HPMB_V. Instead, despite having lower stiffness than PMB, the HPMB_O curve partially overlaps with that of the reference bitumen PMB. When considering the fatigue curves (Fig. 10c), a significant improvement can be observed for the HPMBs compared to the reference

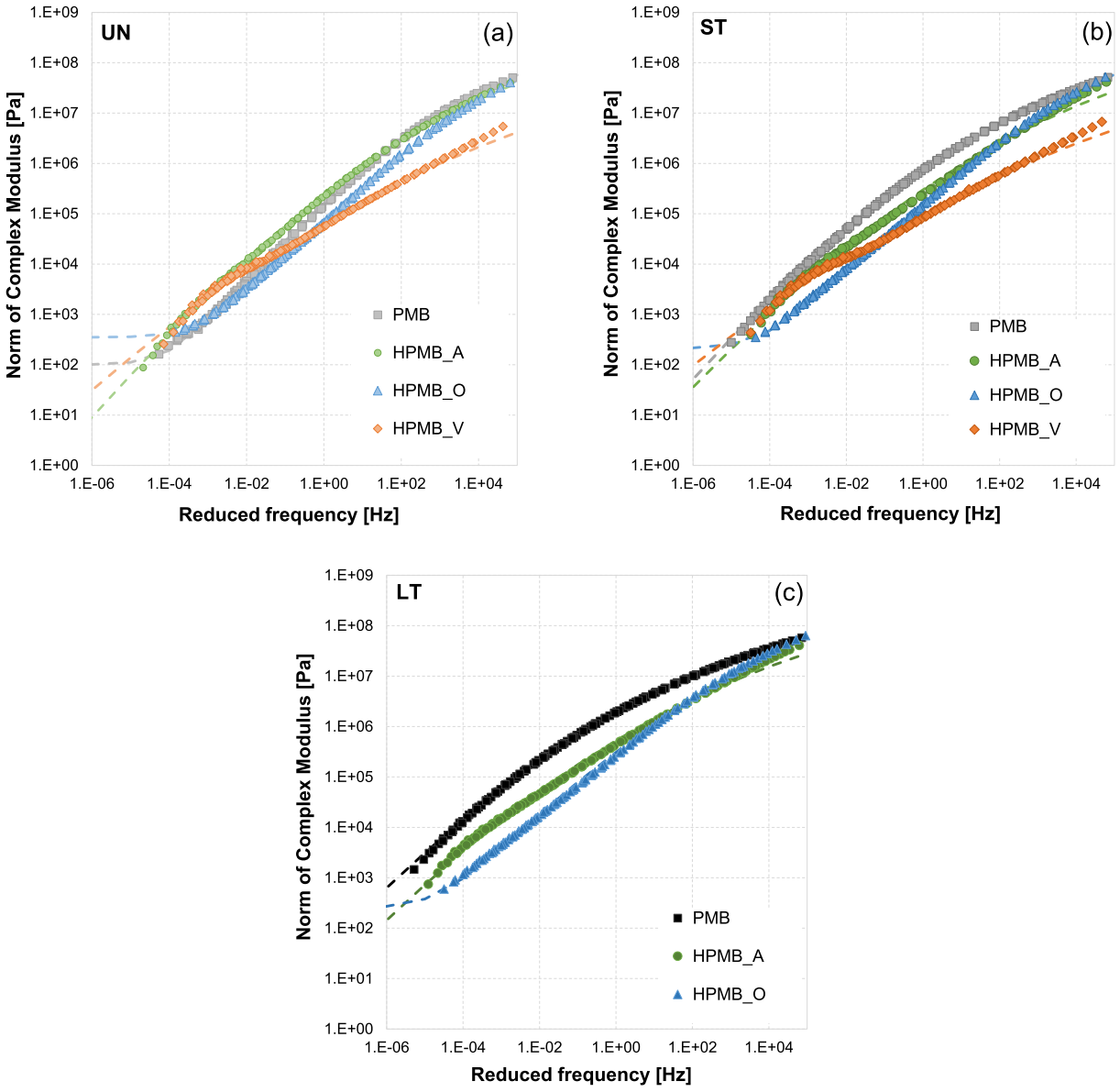

Fig. 7. Master curves of complex modulus norm at the reference temperature of 34 °C (experimental data and modified CAM model): (a) unaged binders, (b) short-term aged binders, (c) long-term aged binders.

bitumen PMB. In particular, the HPMBs show a lower slope of the fatigue curve (parameter *B* in Table 6), resulting in a significantly higher number of cycles to failure at high strain values (range of interest).

A more detailed comparison between the materials can be made by considering the N_f*@15 %* parameter given in Table 6, which represents the number of cycles to failure corresponding to a strain level of 15 %. According to Chen et al. [39], this strain level can be considered representative of the fatigue life of an asphalt binder, because it provides results that are much more consistent with mixture fatigue performance and engineering judgement with respect to those obtained at lower strain levels. The values in Table 6 suggest that the HPMBs have a better fatigue behaviour than the reference bitumen PMB, with a significantly higher N_f*@15 %* value both after short-term aging (+600–700 %) and after long-term aging (+200–400 %). Among the HPMBs, HPMB_A performs better in both aging conditions.

As a result of aging, the parameter *B* increases for all binders (Table 6). Consequently, the long-term aged binders withstand fewer loading cycles compared to the short-term aged binders at medium-high strain levels, as expressed by the N_f*@15 %* values in Table 6. The increase of the parameter *B* indicates a greater sensitivity of the material to the applied strain level [40–43] and is more pronounced for the reference bitumen PMB as compared to the HPMBs.

3.7. *Permanent deformation behaviour*

The values of $R_{3.2}$ and $J_{nr,3.2}$ obtained at the stress level of 3.2 kPa are shown in Fig. 11, as they are considered more significant than the results obtained at 0.1 kPa given the typical high recovery capability of HPMBs [7]. In the figure, the error bars represent the standard deviation.

Fig. 11a shows that the HPMBs generally have higher elastic recovery than the reference bitumen in both aging conditions (unaged and short-term aged). In addition, the elastic recovery tends to be higher under short-term aged conditions than under unaged conditions (a typical result for traditional bitumen due to the stiffening of the material). The strain recovery for HPMB_O is almost 100 % under both aging conditions. In unaged conditions, the elastic recovery of PMB and HPMB_A is similar, whereas HPMB_V shows an intermediate elastic recovery between PMB/HPMB_A and HPMB_O. After short-term aging, the

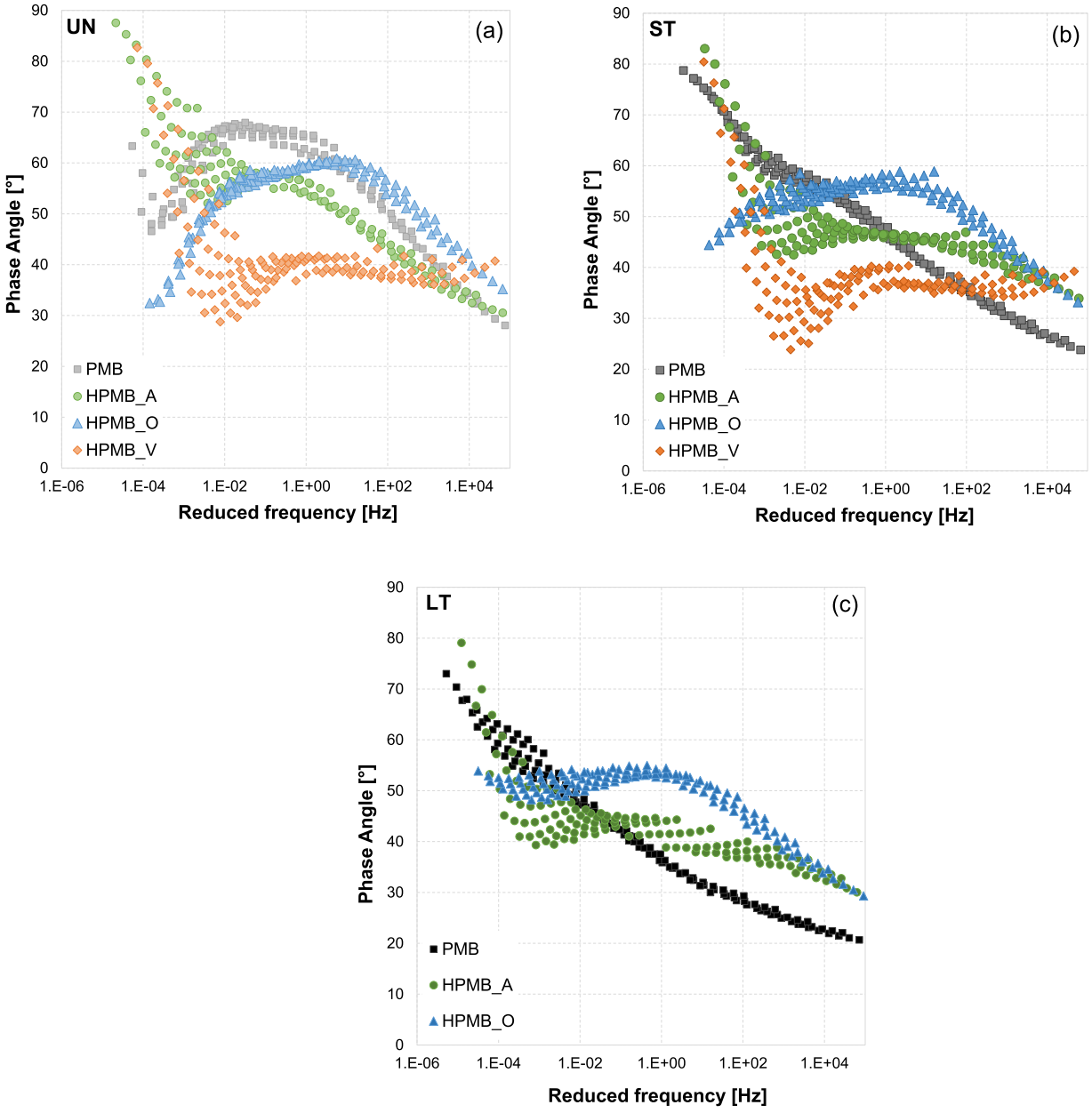

Fig. 8. Master curve of phase angle at the reference temperature of 34 °C (experimental data): (a) unaged binders, (b) short-term aged binders, (c) long-term aged binders.

Table 4
Modified CAM and WLF parameters.

Aging level	Binder	G_g [MPa]	G_e [MPa]	k	m_e	f_c [Hz]	f'_c [Hz]	R	R'	C_1	C_2
Unaged	PMB	10^9	100	0,13	1,00	409	$5•10^{-5}$	2,23	0162	11	112
	HPMB_A	10^9	\	0,11	0,96	66	\	2,68	\	13	130
	HPMB_O	$11•10^9$	350	0,09	0,99	2856	$9•10^{-5}$	3,10	0069	9	102
	HPMB_V	10^9	\	0,06	1,08	0,0032	\	5,49	\	10	119
Short-term aged	PMB	10^9	\	0,10	1,03	1,59		3,03	\	14	133
	HPMB_A	10^9	\	0,09	0,96	0,16	\	3,17	\	11	117
	HPMB_O	$15•10^9$	210	0,09	0,95	1336	$1•10^{-5}$	3,23	0065	13	141
	HPMB_V	10^9	\	0,05	0,97	0,0022	\	5,11	\	13	144
Long-term aged	PMB	10^9	\	0,09	0,99	0,04		3,38	\	17	151
	HPMB_A	10^9	\	0,08	1,03	0,05	\	3,91	\	14	130
	HPMB_O	$7•10^9$	200	0,08	0,95	107	$1•10^{-6}$	3,29	0053	13	130

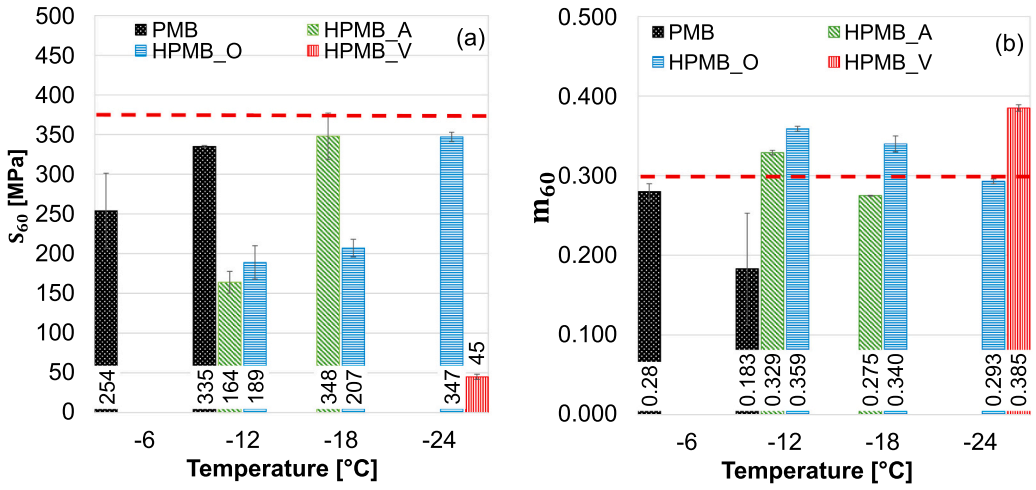

Fig. 9. BBR results: (a) S_{60}, (b) m_{60}.

Table 5
Performance Grade of the binders.

Binder	PG		Continuous PG		$\|G^*\|\bullet\sin\delta$ verification		GRP verification	
	T_{max} [°C]	T_{min} [°C]	T_{max} [°C]	T_{min} [°C]	$T_{fatigue}$ [°C]	$\|G^*\|\bullet\sin\delta$ [kPa]	T_{GRP} [°C]	GRP [kPa]
PMB	76	−10	80,8	$-16 < T_{min} < -10$	37	1085	29	5594
HPMB_A	82	−22	86,3	−26,2	34	354	25	2065
HPMB_O	76	−28	80,8	−31,3	28	684	22	1247
HPMB_V	\	\	$T_{max} > 88$	$T_{min} < -34$	\	\	\	\

same material ranking is observed in terms of $R_{3.2}$: HPMB_O > HPMB_V > HPMB_A > PMB.

The $J_{nr,3.2}$ values shown in Fig. 11b confirm that PMB is more prone to accumulate permanent deformation in both aging conditions (followed by HPMB_A and HPMB_V). As expected, for these binders, aging causes a reduction of $J_{nr3,2}$. HPMB_O, instead, exhibits $J_{nr3,2}$ values close to zero in both aging conditions.

Fig. 11c shows the traffic categories according to AASHTO M 332 [44] based on the $J_{nr,3.2}$ and $J_{nr,diff}$ parameters ($J_{nr,diff}$ is the percentage difference between $J_{nr,3.2}$ and $J_{nr,0.1}$). HPMB_O shows the best permanent deformation resistance and falls into the highest category (Extremely Heavy Traffic, E). As for HPMB_A and PMB (with the same base bitumen), the presence of 7.5 % of styrene polymers with a high vinyl content allows HPMB_A to be classified in the Very Heavy Traffic category (V), whereas PMB is classified in the Heavy Traffic category (H). In the case of HPMB_V, it was not possible to define a traffic category because the value of the $J_{nr,diff}$ parameter exceeds the maximum limit set by the standard [44], which is 75 % (the value of $J_{nr3,2}$ would place this binder in the Extremely Heavy Traffic category (E)).

The improved high-temperature performance observed for the HPMBs compared to the reference bitumen PMB is mainly attributable to their higher polymer content, which leads the material to behave like a "rubber" modified with bitumen (limited accumulation of permanent deformations) rather than a modified bitumen.

It should also be emphasized that the classification of the binders based on MSCR data is not consistent with that based on the conventional SHRP rutting parameter ($|G^*|/\sin\delta$). This is particularly evident for HPMB_O, for which the MSCR data indicate the highest traffic category (E), whereas the verification of the $|G^*|/\sin\delta$ parameter implies a T_{max} similar to that of the reference bitumen PMB (see Table 5). This result suggests that, for complex binders such as those under study, the determination of the PG based on traditional SHRP criteria may not be reliable, as it does not reflect the actual performance of the material.

3.8. Adhesive properties

Fig. 12 shows the average POTS values and failure types for all the studied combinations considering the limestone substrate (Fig. 12a), the basalt substrate (Fig. 12b), the pre-coated limestone substrate (Fig. 12c) and the pre-coated basalt substrate (Fig. 12d). For each combination, the error bars represent the standard deviation.

In general, for all substrates, the average POTS values of the HPMBs are lower compared to PMB, which shows significantly higher POTS values and cohesive failures (C) in both dry and wet conditions. Failure is mainly cohesive (C) for HPMB_O, adhesive (A) for HPMB_A, and undesired (U) and/or adhesive (A) for HPMB_V. In particular, the latter showed problems of adhesion with the metal pull-stubs, leading to undesired (U) failures at the binder/pull-stub interface, analogously to what observed in the LAS tests carried out with the DSR (detachment of the specimen from the DSR plates).

The results obtained indicate that HPMB_A has lower adhesive properties compared to PMB, probably due to the volumetric predominance of the polymer over the bitumen (it can be hypothesized that the adhesive properties mainly depend on the bituminous phase). Therefore, this aspect needs to be paid attention to, as it could have repercussions on the durability and mechanical behaviour of mixtures produced with HPMB_A. HPMB_O shows cohesive failures with significantly lower POTS values compared to PMB, in line with the lower stiffness observed from the rheological tests (see Fig. 7). For HPMB_V, numerous detachments occurred between pull-stub and binder, but the POTS values are similar to those of the other binders. This finding indicates that the adhesion between pull-stub and binder is the weak point of the system, whereas the adhesion between binder and aggregate is certainly higher than the POTS value obtained. Moreover, in general, wet conditioning does not have a significantly negative effect on POTS and failure type. In fact, if HPMB_V is excluded (for which numerous undesired failures were observed), a *t*-test reveals that the difference between dry and wet conditions is not statistically significant in 9 cases out of 12. The only

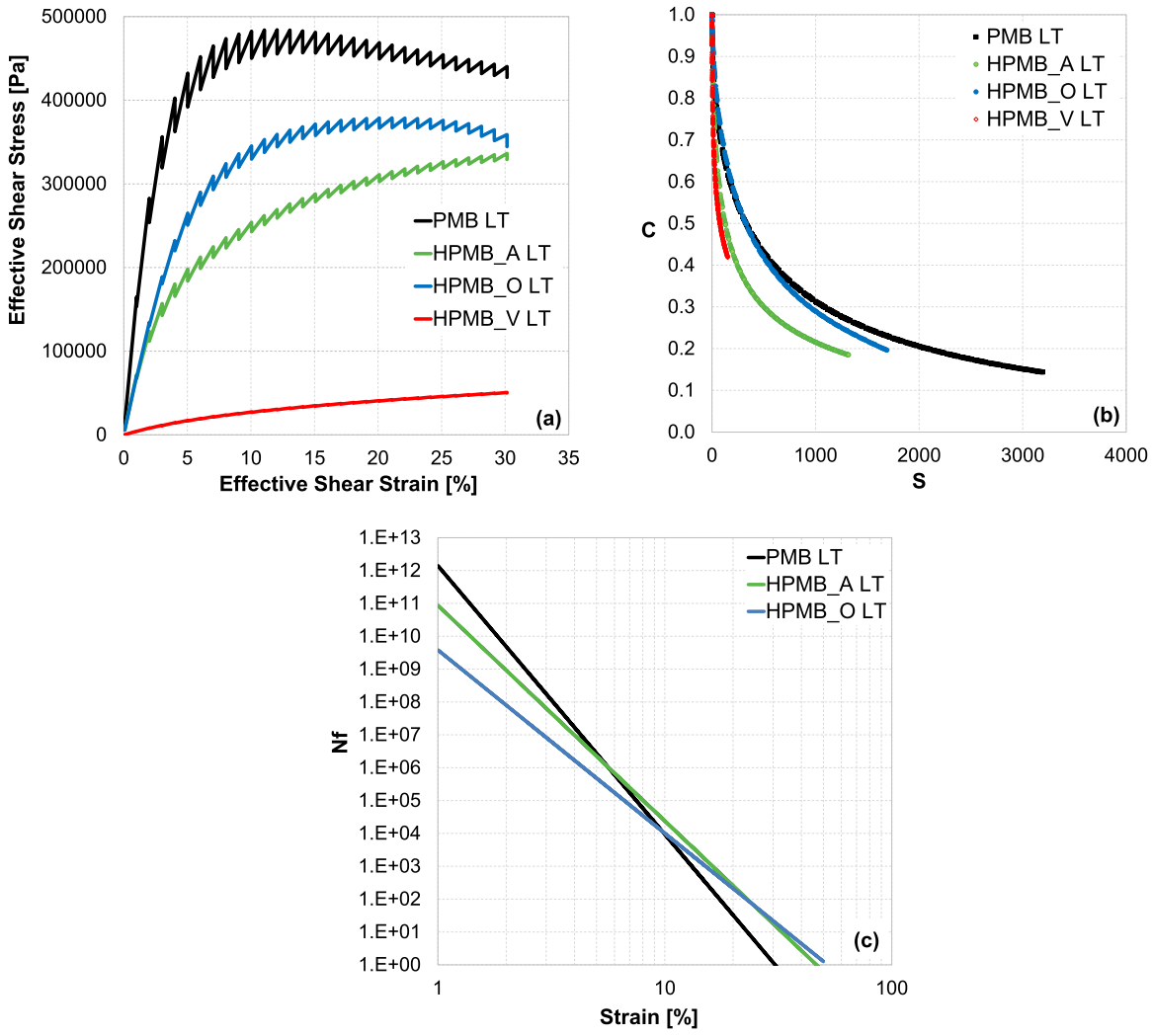

Fig. 10. LAS results for the long-term aged binders: (a) stress-strain curve, (b) damage characteristic curve, (c) fatigue curve.

Table 6
LAS parameters: C_{11}, C_{12}, A_{35}, B, N_f@15 %.

Aging level	Binder	C_{11}	C_{12}	A_{35}	B	N_f@15 %
Short-term aged	PMB	0,105	0,275	3,45E+ 10	6,81	359
	HPMB_A	0,148	0,250	3,82E+ 10	6,05	2893
	HPMB_O	0,065	0,353	3,21E+ 09	5,20	2478
Long-term aged	PMB	0,125	0,242	1,43E+ 12	8,10	340
	HPMB_A	0,165	0,228	8,70E+ 10	6,56	1696
	HPMB_O	0,068	0,338	3,83E+ 09	5,58	1045

exceptions are the binder PMB with pre-coated limestone and the binder HPMB_O with both virgin and pre-coated limestone.

For all studied combinations, there are no substantial differences in terms of POTS between basalt and limestone substrates, regardless of the aggregate condition (virgin or pre-coated) and the specimen conditioning (dry or wet). The only exception is represented by the reference bitumen PMB with pre-coated aggregates under wet conditions. In this case, the POTS in the presence of pre-coated basalt is 26 % lower than in the presence of pre-coated limestone. These findings indicate that the analysed HPMBs show comparable affinity with calcareous and siliceous aggregates, which may be attributed to the volumetric predominance of the polymer over the bitumen. Conversely, in the reference bitumen PMB the bituminous phase remains the predominant one, resulting in lower chemical affinity with basalt (typical behaviour of traditional bitumen).

Finally, for the HPMBs, no significant differences emerge when comparing virgin and pre-coated substrates, indicating the applicability of these binders both in virgin mixtures and in recycled mixtures.

4. Conclusions

This study characterized the chemical, rheological, performance and durability properties of an HPMB currently under development for use in Italian motorway pavements (“HPMB_A”) and compared this binder with a reference PMB and other two HPMBs available on the market (“HPMB_O” and “HPMB_V”). PMB and HPMB_A were produced at large scale using the same base binder and following the same procedure.

The main findings of the study can be summarized as follows:

- The FTIR tests revealed peaks at 699 and 966 cm^{-1} (characteristic of styrene polymers) for all binders, whereas HPMBs also exhibited a peak at 908 cm^{-1} , associated with high-vinyl polybutadiene.
- The viscosity tests suggested that PMB and HPMB_A have comparable workability for both hot (T ≈ 170 °C) and warm (T ≈ 130 °C) productions, mainly due to the common base bitumen and the use of low molecular weight polymers in HPMB_A.
- HPMBs exhibit a more complex rheological behaviour than PMB. HPMB_A and HPMB_V show a ’bump’ in the master curve of the complex modulus norm at medium-low frequencies, corresponding to an inverse "N" shape in the phase angle master curve, possibly due

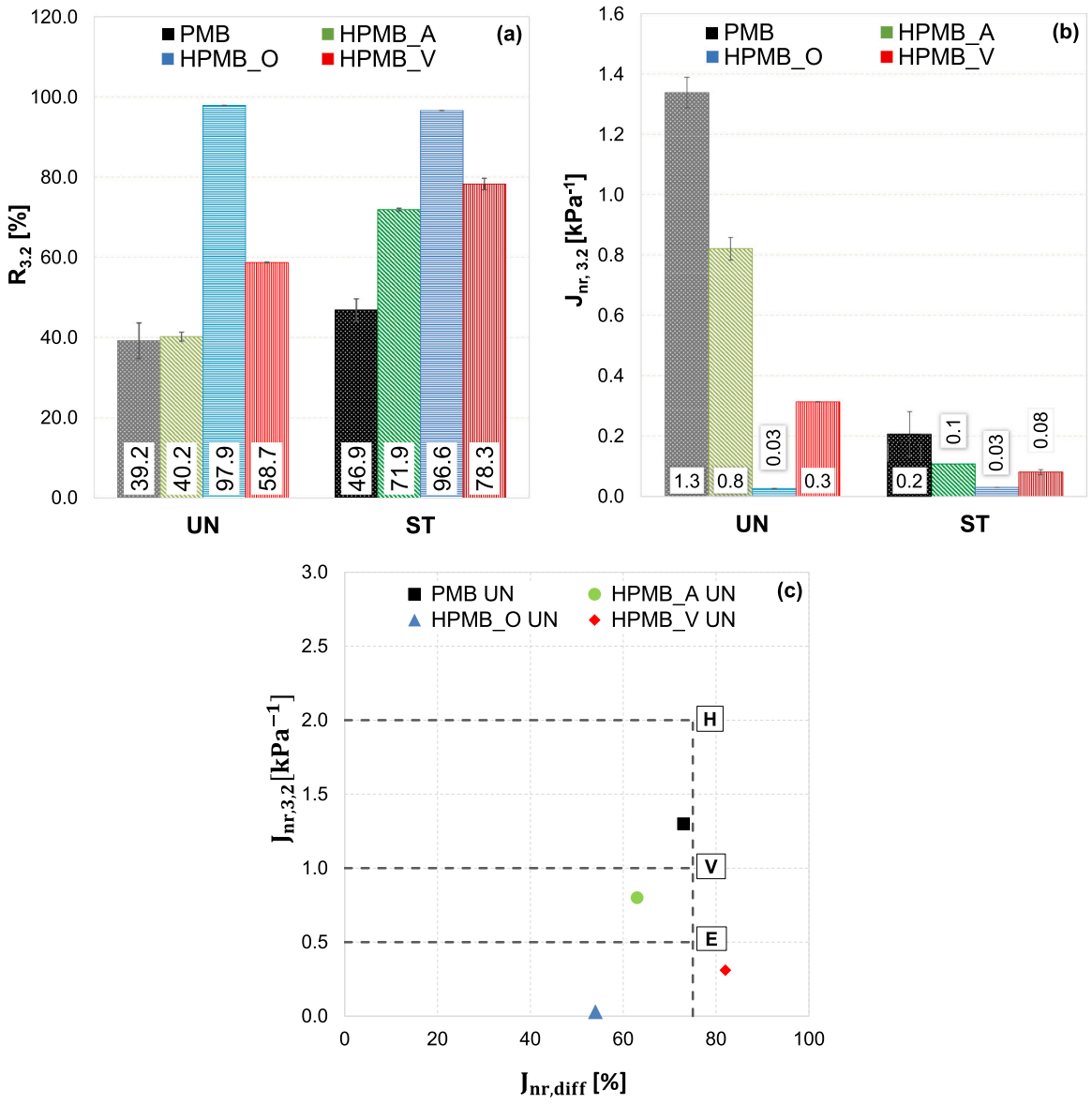

Fig. 11. MSCR results at 70 °C and 3.2 kPa: (a) percent strain recovery, (b) non-recoverable creep compliance, (c) classification of the binders according to AASHTO M 332 [44].

to the dominance of the polymer's behaviour over the bitumen behaviour. HPMB_O behaves more similarly to PMB, with a rubbery asymptote at low frequencies.

- The PG and continuous PG indicate that HPMBs outperform PMB, leading to an extended useful temperature interval (e.g., PG 82–22 for HPMB_A vs. PG 76–10 for PMB).
- The LAS tests revealed that the fatigue resistance of HPMBs is significantly higher than that of PMB, both after short-term aging (+600–700 %) and long-term aging (+200–400 %).
- The MSCR tests demonstrated that HPMBs exhibit an extremely high elastic recovery capability and very low deformability at high service temperatures.
- The superior performance of HPMBs is mainly attributable to their higher polymer content, which makes the material behave like a "rubber" modified with bitumen rather than a modified bitumen, reducing thermo- and time-dependence.
- The BBS tests revealed that HPMBs generally exhibit lower adhesive properties compared to PMB likely due to the volumetric predominance of the polymer over the bitumen, which might impact mixture performance and durability.
- The chemical and mechanical tests highlighted that HPMBs broadly exhibit lower aging susceptibility than PMB, which is attributable to the presence of highly reactive C═C double bonds of polybutadiene in the side chains instead of the main chain. Conversely, HPMB_O exhibits a polymer degradation comparable to PMB.
- The binder classification based on MSCR tests and Glover-Rowe parameter was not entirely consistent with that based on SHRP rutting and fatigue parameters ($|G^*|/\sin\delta$ and $|G^*|\cdot\sin\delta$). For complex binders like HPMBs, conventional tests and performance criteria may not adequately reflect material performance.

In conclusion, the study of the binder phase shows that the performance of the binder under development (HPMB_A) is better than that of PMB (routinely used in asphalt mixtures for Italian motorway pavements). The results are also very promising when compared to other HPMBs already available on the market. Further insights will be possible following the evaluation of the mechanical behaviour of asphalt mixtures produced with the binders investigated in this study (already ongoing).

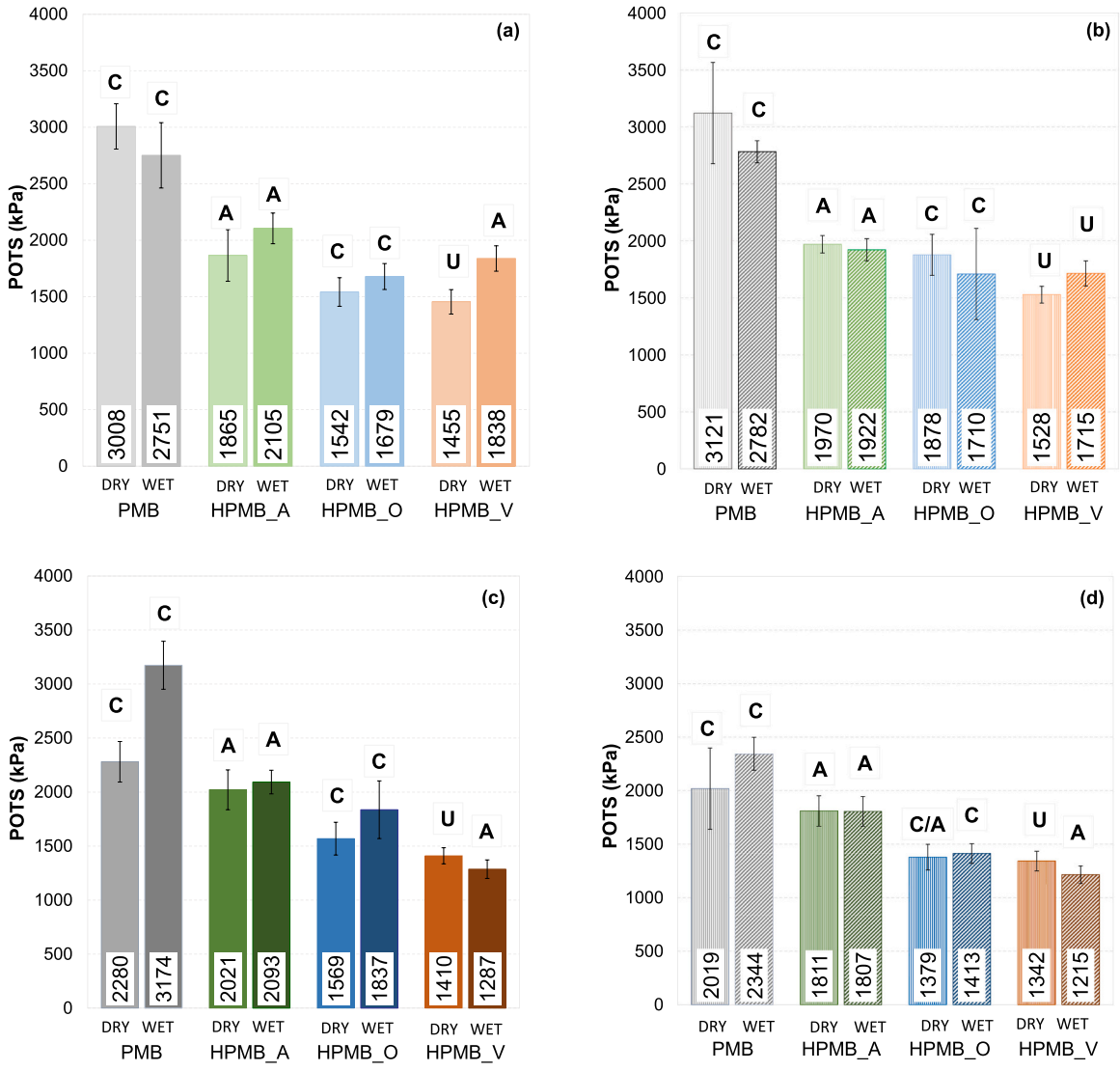

Fig. 12. BBS results: (a) virgin limestone, (b) virgin basalt, (c) pre-coated limestone, (d) pre-coated basalt.

CRediT authorship contribution statement

Francesco Canestrari: Writing – review & editing, Methodology, Formal analysis, Conceptualization. **Andrea Graziani:** Writing – review & editing, Formal analysis. **Simona Sabbatini:** Writing – review & editing, Investigation, Formal analysis. **Lorenzo Paolo Ingrassia:** Writing – original draft, Visualization, Methodology, Formal analysis. **Sara Carlucci:** Writing – original draft, Visualization, Investigation, Formal analysis.

Declaration of Competing Interest

The authors declare that they have no known competing financial interests or personal relationships that could have appeared to influence the work reported in this paper.

Acknowledgements

The activities presented in this paper were sponsored by Amplia Infrastructures S.p.A. (Italy), which gave both financial and technical support. The results and opinions presented are those of the authors.

Data availability

Data will be made available on request.

References

[1] J. Zhu, B. Birgisson, N. Kringos, Polymer modification of bitumen: advances and challenges, Eur. Polym. J. 54 (2014) 18–38.
[2] M. Porto, P. Caputo, V. Loise, S. Eskandarsefat, B. Teltayev, C.O. Rossi, Bitumen and bitumen modification: a review on latest advances, Appl. Sci. 9 (4) (2019) 742.
[3] B. Sengoz, A. Topal, G. Isikyakar, Morphology and image analysis of polymer modified bitumens, Constr. Build. Mater. 23 (5) (2009) 1986–1992.
[4] E.J. Scholten, W. Vonk, J. Korenstra, Towards Green pavements with novel class of SBS polymers for enhanced effectiveness in bitumen and pavement performance, Int. J. Pavement Res. Technol. 3 (4) (2010) 216–222.
[5] O.V. Luksha, O.N. Opanasenko, N.P. Krut'ko, Y.V. Loboda, Modification of oxidized bitumen with Styrene-Butadiene-Styrene copolymers of various structures, Russ. J. Appl. Chem. 79 (6) (2006) 1021–1024.
[6] G. Hernandez, E.M. Medina, R. Sanchez, A.M. Mendoza, Thermomechanical and rheological asphalt modification using Styrene-Butadiene triblock copolymers with different microstructure, Energy Fuels 20 (2006) 2623–2626.
[7] W. Wu, M.C. Cavalli, W. Jiang, N. Kringos, Differing perspectives on the use of high-content SBS polymer-modified bitumen, Constr. Build. Mater. 411 (2024) 134433.
[8] S.S. Islam, S.K. Singh, G.D.R.N. Ransinchung, S.S. Ravindranath, Imperative role of SBS molecular structure on the performance properties of modified binders and asphalt mixes, Int. J. Pavement Eng. 24 (1) (2023) 2226290.

[9] Y. Kumar, A. Pandey, P. Kumar, S.S. Ravindranath, Elevated temperature rheological properties of Styrene-Butadiene-Modified binders: role of molecular structure, Int. J. Pavement Res. Technol. 16 (2023) 1599–1617.
[10] S.K. Singh, Y. Kumar, S.S. Ravindranath, Thermal degradation of SBS in bitumen during storage: influence of temperature, SBS concentration, polymer type and base bitumen, Polym. Degrad. Stab. 147 (2018) 64–75.
[11] J. Habbouche, I. Boz, E.Y. Hajj, N.E. Morian, Influence of aging on rheology- and chemistry-based properties of high polymer-modified asphalt binders, Int. J. Pavement Eng. 23 (10) (2022) 3285–3303.
[12] C. Rivera, S. Caro, E. Arambula-Mercado, D.B. Sanchez, P. Karki, Comparative evaluation of ageing effects on the properties of regular and highly polymer modified asphalt binders, Constr. Build. Mater. 302 (2021) 124163.
[13] M. Elwardany, J. Habbouche, A. Andriescu, D.J. Mensching, E.Y. Hajj, M. Piratheepan, Comprehensive performance evaluation of high polymer-modified asphalt binders beyond linear viscoelastic rheological surrogates, Constr. Build. Mater. 351 (2022) 128902.
[14] EN 12607-1, 2014. Bitumen and Bituminous Binders – Determination of the Resistance to Hardening under Influence of Heat and Air – Part 1: RTFOT method.
[15] EN 14769, 2012. Bitumen and Bituminous Binders – Accelerated Long-term Ageing Conditioning by A Pressure Ageing Vessel (PAV).
[16] B. Hofko, M.Z. Alavi, H. Grothe, D. Jones, J. Harvey, Repeatability and sensitivity of FTIR ATR spectral analysis methods for bituminous binders, Mater. Struct. 50 (2017) 187.
[17] EN 13302, 2018. Bitumen and Bituminous Binders – Determination of Dynamic Viscosity of Bituminous Binder Using A Rotating Spindle Apparatus.
[18] EN 14770, 2012. Bitumen and Bituminous Binders – Determination of Complex Shear Modulus and Phase Angle – Dynamic Shear Rheometer (DSR).
[19] M. Gergesova, B. Zupančič, I. Saprunov, I. Emri, The closed form t-T-P shifting (CFS) algorithm, J. Rheol. 55 (1) (2011) 1–16.
[20] M.L. Williams, R.F. Landel, J.D. Ferry, The temperature dependence of relaxation mechanisms in amorphous polymers and other glass-forming liquids, J. Am. Chem. Soc. 77 (14) (1955) 3701–3707.
[21] Bahia, H.U., Hanson, D.I., Zeng, M., Zhai, H., Khatri, M.A., Anderson, R.M., 2001. Characterization of Modified Asphalt Binders in Superpave Mix Design. National Cooperative Highway Research Program (NCHRP) Report 459. Transportation Research Board, Washington DC (USA).
[22] D.A. Anderson, D.W. Christensen, H.U. Bahia, R. Dongre, M.G. Sharma, C.E. Antle, J. Button, Binder characterization and evaluation, volume 3: physical characterization, SHRP report A-369, strategic highway research program, Natl. Res. Counc. Wash. DC (USA) (1994).
[23] EN 14771, 2023. Bitumen and Bituminous Binders – Determination of the Flexural Creep Stiffness – Bending Beam Rheometer (BBR).
[24] AASHTO M 320, 2023. Standard specification for Performance-Graded Asphalt Binder.
[25] D.W. Christensen, N. Tran, Relationships between the fatigue properties of asphalt binders and the fatigue performance of asphalt mixtures, NCHRP Research Report 982, The National Academies Press, Washington, DC, 2022.
[26] AASHTO T 391, 2020. Estimating Fatigue Resistance of Asphalt Binders Using the Linear Amplitude Sweep.
[27] AASHTO T 350, 2019. Standard Method of Test for Multiple Stress Creep Recovery (MSCR) test of asphalt binder using a Dynamic Shear Rheometer (DSR).
[28] AASHTO T 361, 2022. Method of Test for Determining Asphalt Binder Bond Strength by Means of the Asphalt Bond Strength (ABS) Test.
[29] F. Canestrari, G. Ferrotti, F. Cardone, A. Stimilli, Innovative testing protocol for evaluation of Binder-Reclaimed aggregate bond strength, Transp. Res. Rec. 2444 (1) (2014) 63–70.
[30] AASHTO R 30, 2002. Standard Pract.
[31] Choquet, F.S., Ista, E.J., 1992. The determination of SBS, EVA and APP polymers in modified bitumens. Polymer Modified Asphalt Binders, ASTM STP 1108 Wardlaw, K.R., Shuler, S., Eds., American Society for Testing and Materials, Philadelphia.
[32] P. Marsac, N. Pierard, L. Porot, W. Van den bergh, J. Grenfell, V. Mouillet, S. Pouget, J. Besamusca, F. Farcas, T. Gabet, M. Hugener, Potential and limits of FTIR methods for reclaimed asphalt characterisation, Mater. Struct. 47 (2014) 1273–1286.
[33] L.P. Ingrassia, X. Lu, G. Ferrotti, C. Conti, Investigating the “circular propensity” of road bio-binders: effectiveness in hot recycling of reclaimed asphalt and recyclability potential, J. Clean. Prod. 255 (2020) 120193.
[34] S.K.S. Islam, S.K. Singh, G.D.R.N. Ransinchung, S.S. Ravindranath, Performance degradation during elevated storage temperature of SBS-modified binders and asphalt mixes: impact of SBS molecular structure, J. Mater. Civ. Eng. 35 (3) (2022) 04022457.
[35] P. Lin, C. Yan, W. Huang, Y. Li, L. Zhou, N. Tang, F. Xiao, Y. Zhang, Q. Lv, Rheological, chemical and aging characteristics of high content polymer modified asphalt, Constr. Build. Mater. 207 (2019) 616–629.
[36] E. Chailleux, G. Ramond, C. Such, C. de La Roche, A mathematical-based master curve construction method applied to complex modulus of bituminous materials, Road. Mater. Pavement Des. 7 (sup1) (2006) 75–92.
[37] B. Delaporte, H. Di Benedetto, P. Chaverot, G. Gauthier, Linear viscoelastic properties of bituminous material: from binder to mastic, J. Assoc. Asph. Pavement Technol. 76 (2007) 455–494.
[38] D. Yuan, C. Xing, W. Jiang, J. Xiao, W. Wu, P. Li, Y. Li, Viscoelastic behavior and phase structure of High-Content SBS-Modified asphalt, Polymers 14 (2022) 2476.
[39] H. Chen, Y. Zhang, H.U. Bahia, Modelling asphalt binder fatigue at multiple temperatures using complex modulus and the LAS test, Int. J. Pavement Eng. 23 (13) (2022) 4600–4609.
[40] G. Cuciniello, P. Leandri, M. Losa, G. Airey, Effects of ageing on the damage tolerance of polymer modified bitumens investigated through the LAS test and fluorescence microscopy, Int. J. Pavement Eng. 23 (4) (2022) 1083–1094.
[41] J. Xu, J. Pei, J. Cai, T. Liu, Y. Wen, Performance improvement and aging property of oil/SBS modified asphalt, Constr. Build. Mater. 300 (2021) 123735.
[42] W. Cao, X. Li, Y. Wang, C. Wang, Intermediate and high temperature performance of biobinders with various oxidative aging, J. Mater. Civ. Eng. 31 (12) (2019) 04019300.
[43] H. Chen, H.U. Bahia, Modelling effects of aging on asphalt binder fatigue using complex modulus and the LAS test, Int. J. Fatigue 146 (2021) 106150.
[44] AASHTO M 332, 2023. Standard Specification for Performance-Graded Asphalt Binder Using Multiple Stress Creep Recovery (MSCR) Test.